PHYSICAL REVIEW B **82**, 140508(R) (2010)

Coexistence of localized and itinerant electronic states in the multiband iron-based superconductor $FeSe_{0.42}Te_{0.58}$

D. Arčon,[1,2,*] P. Jeglič,[1] A. Zorko,[1] A. Potočnik,[1] A. Y. Ganin,[3] Y. Takabayashi,[4] M. J. Rosseinsky,[3] and K. Prassides[4]
[1]*Institute "Jozef Stefan," Jamova 39, 1000 Ljubljana, Slovenia*
[2]*Faculty of Mathematics and Physics, University of Ljubljana, Jadranska 19, 1000 Ljubljana, Slovenia*
[3]*Department of Chemistry, University of Liverpool, Liverpool L69 7ZD, United Kingdom*
[4]*Department of Chemistry, Durham University, Durham DH1 3LE, United Kingdom*
(Received 17 June 2010; revised manuscript received 3 September 2010; published 25 October 2010)

We report X-band electron paramagnetic resonance (EPR) and ^{125}Te and ^{77}Se NMR measurements on single-crystalline superconducting $FeSe_{0.42}Te_{0.58}$ [T_c=11.5(1) K]. The data provide indications for the coexistence of intrinsic localized and itinerant electronic states. In the normal state, localized moments couple to itinerant electrons in the Fe(Se,Te) layers and affect the local spin susceptibility and spin fluctuations. Below T_c, spin fluctuations become rapidly suppressed and an unconventional superconducting state emerges in which $1/T_1$ is reduced at a much faster rate than expected for conventional s- or $s_{\pm}$-wave symmetry. We suggest that the localized states arise from the strong electronic correlations within one of the Fe-derived bands. The multiband electronic structure together with the electronic correlations thus determine the normal and superconducting states of the $FeSe_{1-x}Te_x$ family, which appears much closer to other high-T_c superconductors than previously anticipated.

DOI: 10.1103/PhysRevB.82.140508 PACS number(s): 74.70.Xa, 74.25.nj

It is generally accepted that strong electron correlations are responsible for peculiar phase diagrams of high-T_c superconductors where superconductivity (SC) appears in the proximity of antiferromagnetic (AF) Mott insulating phases.[1–3] However, in iron-based superconductors the role of electron correlations is less clear. They are believed to be weaker[4] because the ground state of the parent compounds is metallic with a low-temperature spin-density-wave state induced by the Fermi-surface nesting. Iron-based superconductors have a complicated multiband structure with all five Fe d bands crossing the Fermi level. It has been proposed that differences in the p-d hybridization may lead to the formation of more localized orbitals.[5] Therefore, each band could be affected by electron correlations differently to a degree that an orbital-selective Mott transition may take place.[6,7]

In order to address the problem of electronic correlations and possible carrier localization, we focus on the $FeSe_{0.42}Te_{0.58}$ compound, a member of the layered iron-chalcogenide, FeQ (Q=Se,Te) superconductors. The two end members, $Fe_{1.01}Se$ and $Fe_{1+\delta}Te$ ($\delta \leq 0.14$), exhibit fundamentally different ambient-pressure ground states. $Fe_{1+\delta}Se$ is a superconductor with critical temperature $T_c \sim 9$ K at ambient pressure.[8–10] On the other hand, AF long-range order develops in $Fe_{1+\delta}Te$ below $\sim$65 K with the magnetic order vector $Q_{AF}=(\frac{1}{2},\frac{1}{2})$, the rather large ordered moment exceeding 2 μ_B/Fe and the Curie-Weiss-type susceptibility in the paramagnetic state of $Fe_{1+\delta}Te$ suggesting that the magnetism is of a local-moment origin.[11] In contrast to other Fe-based superconductors, no Fermi-surface instability associated with AF order was observed.[12] Moreover, inelastic neutron-scattering measurements indicate a spin-fluctuation spectrum, which is best described with an identical model to that used for the normal-state spin excitations in the high-T_c cuprates.[13] In addition, an anomalously large mass renormalization, $m^*/m_{band} \approx 6-20$ has been reported recently for $FeSe_{0.42}Te_{0.58}$ from angle-resolved photoemission spectroscopy (ARPES) data,[14] consistent with the high bulk-specific heat coefficient, γ=39 mJ/mol K^2, obtained for a sample with a similar composition $Fe_{1+y}Se_{0.33}Te_{0.67}$.[15] These results highlight the importance of electronic correlations in the FeQ family, which in analogy to other strongly correlated multiband systems may dramatically lower the energy difference between the coherent quasiparticle states and the incoherent excitations with more local character.[14]

Here we report a combined electron paramagnetic resonance (EPR) and ^{77}Se, ^{125}Te NMR study of the $FeSe_{0.42}Te_{0.58}$ superconductor [T_c=11.5(1) K], which provides evidence for the coexistence of two electronic components arising from itinerant and localized states. The coupling between these states at the atomic scale leads to the screening of localized moments and may be responsible for the observed suppression of the AF spin fluctuations. A surprisingly large effective gap $\Delta=3k_BT_c$ is found from the spin-lattice relaxation data. The intrinsic localized states are likely signatures of strong electron correlations making the FeQ family a close relative to other high-T_c superconductors.

The single-crystalline $FeSe_{0.42}Te_{0.58}$ sample used in this work was identical to that of Ref. 14. Hexagonal FeSe [1.27(2)%] and elemental Se [2.31(4)%] were identified as impurities in crushed powders by synchrotron x-ray diffraction measurements (Fig. S1). The bulk magnetic susceptibility, χ_S, was measured with a commercial Quantum Design SQUID magnetometer system on a 0.547 mg single crystal and with the magnetic field applied along the crystal c axis. NMR frequency-swept spectra were measured in a magnetic field of 9.4 T. Details of ^{125}Te and ^{77}Se line-shape and relaxation-time measurements can be found in the supplementary material.[16] For the temperature-dependent X-band (9.6 GHz) cw-EPR experiments, a small piece of the crystal was exfoliated from the large crystal and sealed under dynamic vacuum in a standard silica tube.[16]

The very intense EPR resonance [inset Fig. 1(a)] has been measured at room temperature and is best described by

 ©2010 The American Physical Society

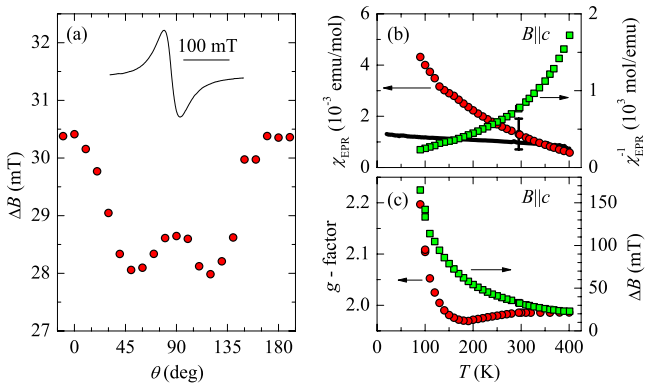

FIG. 1. (Color online) (a) Angular dependence of the room-temperature EPR linewidth in $FeSe_{0.42}Te_{0.58}$ single crystal. $\theta=0$ is the $B\|c$ crystal orientation. Inset: room-temperature EPR spectrum for $B\|c$. Horizontal bar indicates field scale. (b) Temperature dependence of the EPR spin susceptibility, χ_{EPR} (circles, left scale), the bulk spin susceptibility, χ_S (black solid line), and the inverse spin susceptibility, χ^{-1}_{EPR} (squares, right scale). (c) Temperature dependence of the EPR g factor (left scale, circles) and linewidth, ΔB (right scale, squares).

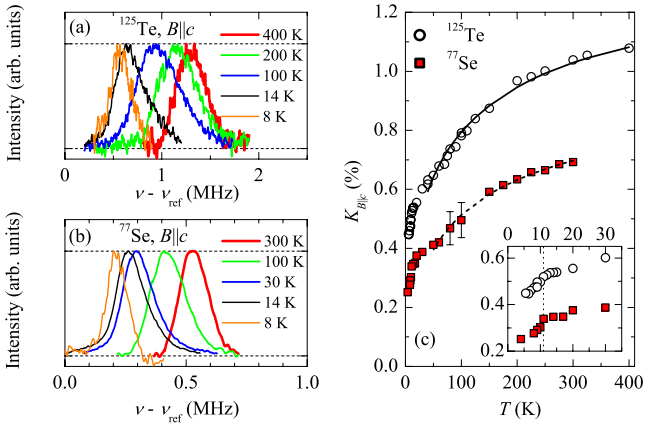

FIG. 2. (Color online) Frequency-swept (a) ^{125}Te and (b) ^{77}Se NMR spectra of $FeSe_{0.42}Te_{0.58}$ single crystal measured with $B\|c$. (c) Temperature dependence of the ^{125}Te (^{125}K, open circles) and ^{77}Se (^{77}K, solid squares) Knight shifts. The lines are fits to the model described in the text. Inset: expanded region near $T_c=11.5(1)$ K, showing the clear drop of ^{125}K and ^{77}K.

Dyson line shape as expected for metallic samples. At 300 K, the calibrated EPR intensity corresponds to a spin susceptibility, $\chi_{EPR}=1.3(5)\times10^{-3}$ emu/mol—the large uncertainty in the value of χ_{EPR} arises from difficulties in the precise positioning of the tiny single crystal in the resonator—which is comparable to the measured $\chi_S=1.0(1)\times10^{-3}$ emu/mol [Fig. 1(b)] and to that reported for $FeTe_{0.55}Se_{0.45}$.[15] The negligibly small refined content of Fe interstitials between the Fe(Se/Te) slabs[14,16] cannot be responsible for the measured χ_{EPR}. On the other hand, hexagonal $FeSe_{1-x}$ phases can be ferromagnetic with Curie temperatures exceeding room temperature[17] and could give rise to strong ferromagnetic resonance. However, since the hexagonal $FeSe_{1-x}$ magnetization is already fully saturated in the field of the EPR resonance (~0.33 T), we conclude that it cannot account for the strong temperature dependence of χ_{EPR} [Fig. 1(b)].[16] We thus tentatively suggest that the measured EPR signal is *intrinsic*.

The EPR resonance shows a strong angular dependence of the EPR linewidth, ΔB. The minima in ΔB at angles $\theta_m \sim 54°$ and ~126° when the crystal is rotated away from the $B\|c$ orientation [Fig. 1(a)] are unexpected for a conduction electron-spin resonance[18] but may indicate the dipolar interactions between the exchange-coupled localized moments.[19] The presence of states with more local character is further supported by the temperature dependence of χ_{EPR}, which rapidly increases with decreasing temperature [Fig. 1(b)]. However, the nonlinear dependence of the inverse EPR susceptibility between 100 and 400 K [Fig. 1(b)] is not consistent with the simple Curie-Weiss law expected for localized moments only, implying that the measured EPR signal has contributions from both quasiparticle and localized states. Simple macroscopic phase segregation into metallic and insulating fractions would have implied that χ_{EPR} can be expressed as $\chi_{EPR}=\chi_c+\chi_l$, where χ_c is the spin susceptibility of quasiparticles, which is expected to be only weakly temperature dependent and χ_l is the spin susceptibility of localized states. But this approach results in unphysical parameters (negative χ_c), thus leading to the conclusion that both electronic components not only coexist at the nanometric or atomic scale but that they are also strongly coupled. Such coupling could be responsible for the rapid increase in ΔB and g factor with decreasing temperature [Fig. 1(c)], which indicates development of internal magnetic fields sensed by localized moments. It could also account for another surprising observation: namely, $\chi_{EPR}(T)$ is larger than the weakly temperature-dependent χ_S below room temperature [Fig. 1(b)]. If the coupling is strong enough, then localized states polarize conduction electrons and reduce the effective moment measured in bulk experiments.

To confirm these hypotheses, we employed the NMR local probe technique, which can provide insight on the coexisting electronic components at different scales. Detailed structural characterization[16] rules out intrinsic Fe interstitial impurities and reveals only a very small fraction of extrinsic impurities in the ~1% range that cannot influence the NMR data. Figures 2(a) and 2(b) show the ^{125}Te and ^{77}Se NMR spectra recorded for $B\|c$. The room-temperature linewidths of ^{125}Te and ^{77}Se resonances, $\delta\,^{125}\nu_{1/2}\approx420$ kHz and $\delta\,^{77}\nu_{1/2}\approx130$ kHz, respectively, imply that the local-site structural inhomogeneities resulting from the statistical Se/Te site occupation slightly broaden the ^{125}Te and ^{77}Se NMR spectra, e.g., with respect to the ^{77}Se NMR linewidth measured for $Fe_{1.01}Se$.[20] For comparison, $\delta\,^{77}\nu_{1/2}$ is similar to that in $FeSe_{0.92}$.[21] Interestingly, the ratio, $\delta\,^{125}\nu_{1/2}/\delta\,^{77}\nu_{1/2}\approx3.2$ is significantly larger than that of the corresponding gyromagnetic ratios, $^{125}\gamma/\,^{77}\gamma=1.65$.

The room-temperature NMR spectra are strongly shifted to higher frequencies with respect to the reference. The Knight shifts are $^{125}K=1.04(6)\%$ and $^{77}K=0.69(3)\%$ for ^{125}Te and ^{77}Se nuclei, respectively. The resonances shift considerably to lower frequencies with decreasing temperature [Fig. 2(c)]: $\Delta\,^{125}K=-0.524\%$ and $\Delta\,^{77}K=-0.316\%$ between 300 and 20 K. A similar decrease in ^{77}K has been reported for $Fe_{1.01}Se$ and $Fe_{1.04}Se_{0.33}Te_{0.67}$.[20,22] However, the Knight shifts, ^nK ($n=77,125$) do not scale with the bulk spin sus-

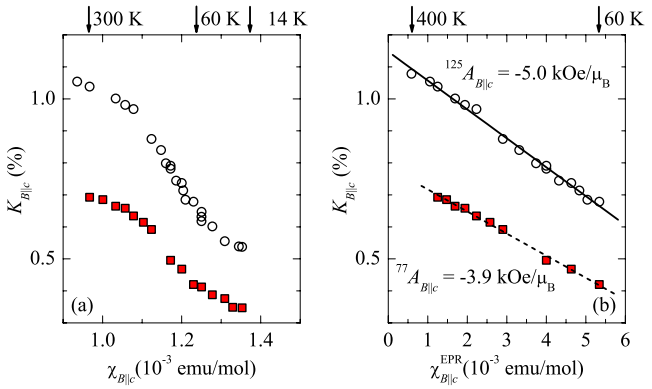

FIG. 3. (Color online) ^{125}K and ^{77}K Knight shifts versus (a) bulk susceptibility, $\chi_{B\|c}$ and (b) χ_{EPR} with temperature as an implicit parameter.

ceptibility over the entire temperature range [Fig. 3(a)]. NMR data thus provide direct evidence that the local and bulk spin susceptibilities are different in the investigated sample. On the other hand, comparing ^{n}K with χ_{EPR}, which also measures the local spin susceptibility, reveals excellent linear scaling [Fig. 3(b)]. If we express the temperature-dependent spin part of the Knight shift as $^{n}K(T)=\frac{^{n}A_{B\|c}}{N_A\mu_B}\chi_{\mathrm{EPR}}$, we derive the coupling constants, $^{125}A_{B\|c}=-5.0(5)$ kOe/μ_B and $^{77}A_{B\|c}=-3.9(8)$ kOe/μ_B. Since we scale ^{n}K with the local rather than the bulk spin susceptibility, the coupling constants are different from those extracted for $Fe_{1.04}Se_{0.33}Te_{0.67}$ only from low-temperature (<100 K) data.[22]

The scaling of ^{n}K with the local rather than with the bulk spin susceptibility is a strong indication for the coexistence of coupled localized and itinerant states at the atomic scale. In the case of two coupled spin components, there are generally three contributions to the spin part of the Knight shift, $^{n}K_S=^{n}K_c+^{n}K_l+^{n}K_{ex}$. Here $^{n}K_c$ stands for the coupling of Te/Se nuclei to the itinerant electrons via hyperfine coupling interaction and should be only weakly temperature dependent, $^{n}K_l$ describes the interaction with the localized states and $^{n}K_{ex}$ is the additional Knight shift arising from the spin-density polarization due to the interaction between the localized and itinerant states. $^{n}K_{ex}$ should be negative in sign,[23] as it is indeed observed. It is intriguing that the strong temperature dependence of ^{n}K can be simulated with the expression $^{n}K\propto[1-(T/T^*)]\log(T^*/T)$, which has been applied to a number of Kondo lattice materials.[24] Here T^* is the correlated Kondo temperature and is a measure of the intersite localized state interactions.[24] Excellent agreement with the experimental data for both nuclei [Fig. 2(b)] is obtained with the same $T^*\sim 800$ K, which falls within the 50–80 meV range of the crossover energy between quasiparticle states and excitations with local character.[14]

The most important experimental finding of this work is that in $FeSe_{0.42}Te_{0.58}$ intrinsic states with localized character may form, coexist and couple with itinerant states. It is suggested that in such strongly correlated systems this coupling plays a vital role in suppressing magnetism and promoting high-temperature superconductivity.[25] Therefore, in order to test the suppression of spin fluctuations we turn to the spin-

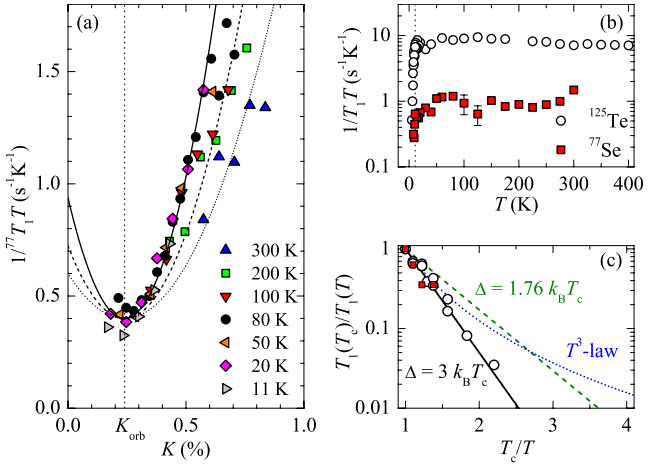

FIG. 4. (Color online) (a) Frequency dependence of $1/^{77}T_1T$ measured at various temperatures (bottom). All measurements fall on the same curve, which scales as $(^{77}K-^{77}K_{orb})^2$ with $^{77}K_{orb}=0.24(3)\%$. Dotted, dashed, and solid lines are calculated curves for $\beta=4$, 2.5, and 1.5, respectively. (b) Temperature dependence of ^{125}Te (open circles) and ^{77}Se (solid squares) $1/^{n}T_1T$ rates. (c) Temperature dependence of $T_1(T_c)/T_1(T)$ below $T_c=11.5(1)$ K. The rate of suppression of $1/T_1$ below T_c is significantly larger than expected for BCS-type superconductivity.

lattice relaxation time, $^{n}T_1$ data, which probe the dynamic spin susceptibility $\chi''(\mathbf{q},\omega)$. Figure 4(a) shows the frequency dependence of $1/^{77}T_1T$ for ^{77}Se NMR spectra at selected temperatures. It is evident that $1/^{77}T_1T$ substantially varies over the ^{77}Se NMR line and the ratio between largest and shortest $1/^{77}T_1T$ measured for the low- and high-frequency spectral shoulders can be as large as 4 (see, for instance, 80 K data). Therefore, a simple two relaxation-times model earlier applied[22] to $Fe_{1.04}Se_{0.33}Te_{0.67}$ oversimplifies the experimental situation and may even lead to erroneous conclusions. $1/^{77}T_1T$ values fall on nearly the same universal Knight shift-dependent curve described by the Korringa relation, $^{77}T_1T\ ^{77}K_S^2=\frac{\hbar}{4\pi k_B}\frac{\gamma_e^2}{\gamma_{Se}^2}\beta$. Here γ_e and γ_{Se} are the electron and nuclear gyromagnetic ratios, respectively. $^{77}K_S$ is given by $^{77}K_S=^{77}K-^{77}K_{orb}$, where $^{77}K_{orb}=0.24(3)\%$ is a temperature-independent orbital shift determined from the fit to the above expression [Fig. 4(a)]. A phenomenological parameter, β characterizes the extent of spin fluctuations and has been recently studied in the context of the normal-state properties of iron-based superconductors. For coupling to noninteracting Fe $3d$ electrons via isotropic transferred hyperfine coupling, β should approach a value of 4.[26] In the case of $FeSe_{0.42}Te_{0.58}$ we find that β gradually decreases from the high-temperature value of 4 to $\sim$1.5 at low temperatures close to T_c and this may thus explain the nearly temperature independent $1/^{n}T_1T$ [Fig. 4(b)]. These values are significantly larger than $\beta\sim 0.1$ found in the LiFeAs superconductor with strong AF spin fluctuations[26] and thus suggest the absence of any significant AF spin fluctuations in the investigated sample. These findings are in striking contrast to FeSe, which clearly shows strong enhancement of AF spin fluctuations toward T_c.[20] Apparently spin fluctuations become suppressed upon Te substitution and are only visible again after the application of pressure.[27] This is fully consis-

tent with the present picture of strong local Kondo effects where local magnetic moments become screened.

Last, we turn to the ^{125}Te and ^{77}Se NMR data below $T_c = 11.5(1)$ K. The ^{125}Te resonance suddenly becomes narrower and more symmetric while its intensity starts to decrease [Fig. 2(a)]. The abrupt decrease in the signal intensity is due to the Meissner shielding of the rf pulses. On the other hand, the sudden decrease in the linewidth is more surprising. In the singlet superconducting state, we expect χ_S to vanish and therefore any broadening and extra resonance shift caused by the interaction between the localized and superconducting states should be reduced below T_c. ^{125}K and ^{77}K suddenly start to decrease at faster rate below T_c [inset Fig. 2(b)], thus indicating the vanishing spin susceptibility as expected both for *s*- and *d*-wave pairing. This is further supported by the $^nT_1$ data. $^nT_1^{-1}$ values are strongly reduced below T_c for both nuclei [Fig. 4(c)]. We also note that $1/T_1$ does not show a coherence peak which has been also missing in FeSe (Ref. 20) and other Fe-based superconductors.[21,28,29] $1/^nT_1$ is exponentially suppressed below T_c with a large effective gap, $\Delta = 3k_BT_c$ being in excellent agreement with that found by point-contact Andreev-reflection spectroscopy ($\Delta = 3.1k_BT_c$).[30] Experimentally, for Fe-pnictide superconductors, $T^{2.5-3}$ dependence has been reported even close to T_c by various groups.[29,31,32] However, for $FeSe_{0.42}Te_{0.58}$ a fit with $\Delta = 3k_BT_c$ is superior over T^3 dependence at least down to $T_c/T = 2.25$. Experiments at even lower temperatures are needed in order to understand if the observed dependence reflects a two-gap case,[31,32] considerable anisotropy of the SC gap[33] or is due to strong-coupling SC with *s*-wave order-parameter symmetry.[30]

The detection of intrinsic localized moments coupled to itinerant electrons shows some similarities with strongly correlated electron systems. The question to resolve is, how these localized states form in $FeSe_{0.42}Te_{0.58}$. Orbitally selective Mott localization has been recently proposed[7] for Fe-based superconductors. This model could well explain the strong local-moment screening implied by the nonscaling of magnetic-resonance parameters with bulk spin susceptibility (Figs. 1 and 3, Fig. S3) and suppression of AF fluctuations in the normal state as well as the ^{125}Te and ^{77}Se NMR data below T_c. The coexisting magnetic and superconducting order parameters on the atomic scale that have been recently suggested for FeSe from μSR experiments[34] is also consistent with this picture. All these results point to the importance of strong intraband electronic correlations which may explain the rapid suppression of $1/T_1$ below T_c, the strong sensitivity of $FeSe_{1-x}Te_x$ superconductivity both to chemical substitution and applied pressure[35–38] and the induced static magnetic order at pressures exceeding 1 GPa.[34]

In conclusion, we have carried out EPR and NMR studies of $FeSe_{0.42}Te_{0.58}$ single crystal. We found indications for the presence of intrinsic localized states coupled to quasiparticles. The possible existence of localized states may be responsible for the suppression of AF spin fluctuations and the surprisingly large effective gap $\Delta = 3k_BT_c$ obtained from the spin-lattice relaxation data in the SC state. Although the exact origin of localized states should be investigated in the future, the present picture is consistent with the intraband electronic correlations leading to a localization of one of the Fe-derived bands. In this respect, the Fe*Q* family appears to be much closer to other high-T_c superconductors and should be treated on a similar footing.

This work was supported in part by the Slovenian research agency through project No. J1-2284-1. P.J. and A.Z. acknowledge support from the Centre of Excellence EN→FIST, Dunajska 156, SI-1000 Ljubljana, Slovenia.

*denis.arcon@ijs.si

[1] P. A. Lee *et al.*, Rev. Mod. Phys. **78**, 17 (2006).
[2] Y. Takabayashi *et al.*, Science **323**, 1585 (2009).
[3] A. Y. Ganin *et al.*, Nature (London) **466**, 221 (2010).
[4] W. L. Yang *et al.*, Phys. Rev. B **80**, 014508 (2009).
[5] J. Wu *et al.*, Phys. Rev. Lett. **101**, 126401 (2008).
[6] L. de' Medici *et al.*, Phys. Rev. Lett. **102**, 126401 (2009).
[7] L. de' Medici *et al.*, J. Supercond. Novel Magn. **22**, 535 (2009).
[8] F.-C. Hsu *et al.*, Proc. Natl. Acad. Sci. U.S.A. **105**, 14262 (2008).
[9] S. Margadonna *et al.*, Chem. Commun. (Cambridge) **2008**, 5607.
[10] T. M. McQueen *et al.*, Phys. Rev. B **79**, 014522 (2009).
[11] S. Li *et al.*, Phys. Rev. B **79**, 054503 (2009).
[12] Y. Xia *et al.*, Phys. Rev. Lett. **103**, 037002 (2009).
[13] M. D. Lumsden *et al.*, Nat. Phys. **6**, 182 (2010).
[14] A. Tamai *et al.*, Phys. Rev. Lett. **104**, 097002 (2010).
[15] B. C. Sales *et al.*, Phys. Rev. B **79**, 094521 (2009).
[16] See supplementary material at http://link.aps.org/supplemental/10.1103/PhysRevB.82.140508 for sample preparation, characterization, and measurement details.
[17] T. Kamimura and T. Iwata, J. Phys. Soc. Jpn. **45**, 1769 (1978).
[18] See for instance S. E. Barnes, Adv. Phys. **30**, 801 (1981).
[19] See, for instance, A. Bencini and D. Gatteschi, *EPR of Exchange Coupled Systems* (Springer-Verlag, Berlin, 1990), p. 149.
[20] T. Imai *et al.*, Phys. Rev. Lett. **102**, 177005 (2009).
[21] H. Kotegawa *et al.*, J. Phys. Soc. Jpn. **77**, 113703 (2008).
[22] C. Michioka, *et al.*, Phys. Rev. B **82**, 064506 (2010).
[23] J. B. Boyce and C. P. Slichter, Phys. Rev. B **13**, 379 (1976).
[24] N. J. Curro *et al.*, Phys. Rev. B **70**, 235117 (2004).
[25] F. J. Ohkawa, J. Phys. Soc. Jpn. **61**, 4490 (1992).
[26] P. Jeglič *et al.*, Phys. Rev. B **81**, 140511(R) (2010).
[27] Y. Shimizu *et al.*, J. Phys. Soc. Jpn. **78**, 123709 (2009).
[28] F. Ning *et al.*, J. Phys. Soc. Jpn. **77**, 103705 (2008).
[29] Y. Nakai *et al.*, J. Phys. Soc. Jpn. **77**, 073701 (2008).
[30] W. Park *et al.*, arXiv:1005.0190 (unpublished).
[31] H.-J. Grafe *et al.*, Phys. Rev. Lett. **101**, 047003 (2008).
[32] S. Kawasaki *et al.*, Phys. Rev. B **78**, 220506 (2008).
[33] D. F. Smith and C. P. Slichter, Lect. Notes Phys. **684**, 243 (2006).
[34] M. Bendele *et al.*, Phys. Rev. Lett. **104**, 087003 (2010).
[35] S. Margadonna *et al.*, Phys. Rev. B **80**, 064506 (2009).
[36] S. Medvedev *et al.*, Nature Mater. **8**, 630 (2009).
[37] Y. Mizuguchi *et al.*, Appl. Phys. Lett. **94**, 012503 (2009).
[38] N. C. Gresty *et al.*, J. Am. Chem. Soc. **131**, 16944 (2009).